



LAWRENCE
LIVERMORE
NATIONAL
LABORATORY

LLNL-TR-679746

Evaluating a Contribution of the Knock-on Deuterons to the Neutron Yield in the Experiments with Weakly Collisional Plasma Jets (Part 1)

D. D. Ryutov

December 1, 2015

Disclaimer

This document was prepared as an account of work sponsored by an agency of the United States government. Neither the United States government nor Lawrence Livermore National Security, LLC, nor any of their employees makes any warranty, expressed or implied, or assumes any legal liability or responsibility for the accuracy, completeness, or usefulness of any information, apparatus, product, or process disclosed, or represents that its use would not infringe privately owned rights. Reference herein to any specific commercial product, process, or service by trade name, trademark, manufacturer, or otherwise does not necessarily constitute or imply its endorsement, recommendation, or favoring by the United States government or Lawrence Livermore National Security, LLC. The views and opinions of authors expressed herein do not necessarily state or reflect those of the United States government or Lawrence Livermore National Security, LLC, and shall not be used for advertising or product endorsement purposes.

This work performed under the auspices of the U.S. Department of Energy by Lawrence Livermore National Laboratory under Contract DE-AC52-07NA27344.

Technical note

November 25, 2015

Evaluating a contribution of the knock-on deuterons to the neutron yield in the experiments with weakly collisional plasma jets (part 1)

D.D. Ryutov

Lawrence Livermore National Laboratory, Livermore, CA 94550

1. Introduction

Laser-generated interpenetrating plasma jets are widely used in the studies of collisionless interaction of counter-streaming plasmas in conjunction with possible formation of collisionless shocks (e.g., Ref. 1). In a number of experiments of this type the plasma is formed on plastic targets made of CH or CD. As was recognized at the very beginning of these studies, the study of the DD neutron production from the interaction between two CD jets on the one hand and between a CD jet and a CH jet could serve as a qualitative indicator of the collisionless shock formation. This concept has been described in a series of internal memos of 2010-2011 and published in Ref. 1 (see the paragraph below Eq. (1) of that paper).

Although a lot of effort has been directed towards making the collisions between the inter-penetrating streams as weak as possible, it turned out to be difficult to make them decisively negligible. Some level of collisions is always present and may contribute to the interaction between the streams. The purpose of this memo is a discussion of the effect of collisions on the neutron generation in the interpenetrating CH and CD jets. Ideally, if the collisions were entirely missing, and the collisionless shock was not formed, the jets should have freely penetrated through each other without producing any neutrons. If the collisions are present but weak, then the CD jet would be somewhat heated by the small-angle scattering on the carbon ions of the counter-propagating CH jet. However, the temperature of the CD jet would remain low and the neutron yield would have stayed negligible. The reason for this statement is that the Coulomb collisions are dominated by the small-angle scattering, so that the collision operator is “almost” a Fokker-Planck, diffusive operator. This in turn means that for a weak collisions there will be no high-energy tails of the distribution function that actually contribute to the neutron yield. We remind that, as there are no deuterons in the counter-propagating stream, the intra-jet deuterium collisions would be the only source of the neutrons.

Here, however, another type of collisions, those associated with small impact parameters, may come into play. Usually they are neglected due to a small cross-section, but here they may instantaneously produce fusing deuterons. The interaction scenario, in a qualitative way, can be characterized as follows. Consider a nearly head-on collision of the deuteron of the CD stream with a carbon of the counter-propagating CH stream. The velocities of the particle in both streams are equal and directed oppositely. The common

value of the velocities is denoted below as V . Elementary momentum and energy conservation arguments show that the velocity of a deuteron after the reflection will be equal to

$$v_{D2} = \frac{3m_C - m_D}{m_C + m_D} V \quad (1)$$

and will be directed along the CH flow. Here and below we use the subscript “2” to denote the parameters after collision. This deuteron then collides head-on with the incoming deuterons of the CD stream, so that the relative collision velocity is

$$v_{rel} = \frac{4m_C}{m_C + m_D} V = \frac{24}{7} V. \quad (2)$$

Note that this velocity is significantly higher than the relative velocity of the counter-propagating deuterons in the CD-CD case, which is $2V$. This boosts the cross-section of neutron-generating collisions and partially compensates for the small value of the Rutherford cross-section for head-on collisions.

Below we will consider the corresponding effects in more detail. First, we discuss the kinematics of the large-deflection collisions of the deuterons and carbon. Then we relate the scattering angles with the corresponding Rutherford cross-section. After that we provide expression for the number of the backscattered deuterons and evaluate their contribution to the neutron yield. The results may be of some significance to the kinetic codes benchmarking and developing the neutron diagnostic.

To put this study in the context of the earlier works on the large-angle scattering, we mention the applications to mirror physics [2], as well as to the diagnostics of the alpha-particle population in a fusing MFE plasmas [3, 4, 5]. The knock-on collisions with the alphas are discussed also in the context of the inertial confinement [6] and development of the Monte-Carlo codes [7].

2. Kinematics of the C-D collisions

In this section we relate the center-of-mass (COM) scattering angle of the D ion with its velocity after collision. Initially both ions are moving along the axis z , the carbon ion to the left, and the deuterium ion to the right. The velocity of the COM frame is equal to

$$u = \frac{m_C - m_D}{m_C + m_D} V \quad (3)$$

The deuteron initial velocity in the COM frame is directed to the left and is equal by the absolute value to

$$v'_{D1} = V + u = \frac{2m_C}{m_C + m_D} V \quad (4)$$

The subscripts “1” and “2” below correspond to the parameters before and after collision. The prime denotes quantities in the COM frame.

The picture of the deuteron scattering in the COM frame is illustrated by Fig. 1. In this frame the velocity vector of the scattered deuterons has the same absolute value as the initial velocity but is turned by some angle (see Ref. 8). We are interested in a large-angle scattering that would correspond to small-to-modest values of χ . The small-angle

scattering (that does not contribute to the effects of interest for us would correspond to χ close to π . With this observations made, one obtains the following expression for the velocity components of the scattered deuteron in the COM frame:

$$\begin{aligned} v'_{zD2} &= \frac{2m_C}{m_C + m_D} V \cos \chi; \\ v'_{\perp D2} &= \frac{2m_C}{m_C + m_D} V \sin \chi. \end{aligned} \quad (5)$$

In the Lab frame the corresponding velocity components are

$$\begin{aligned} v_{zD2} &= \frac{2m_C}{m_C + m_D} V \cos \chi + u = \frac{m_C(2 \cos \chi + 1) - m_D}{m_C + m_D} V; \\ v_{\perp D2} &= \frac{2m_C}{m_C + m_D} V \sin \chi. \end{aligned} \quad (6)$$

The absolute value of the relative velocity of the scattered deuteron and the incoming deuterons of the CD stream is:

$$v_{Drel} = \sqrt{(v_{zD2} + V)^2 + v_{\perp D2}^2} = V \frac{2\sqrt{2}m_C}{m_C + m_D} \sqrt{1 + \cos \chi} \quad (7)$$

For the direct head-on collision with $\chi \rightarrow 0$ this result coincides with Eq. (2). A scattering angle χ in the COM frame can be related to the angle ϑ between the axis z and the velocity of the scattered deuteron in the laboratory frame:

$$\tan \vartheta = \frac{2\sqrt{2} \sin \chi}{2 \cos \chi + 1 - (m_D / m_C)} \quad (8)$$

We present this result for reference only; we will not use it in this report.

3. Rutherford cross-section and the distribution function of scattered deuterons

The differential cross-section is evaluated, in particular, in Ref. 7, Eq. (19.3):

$$d\sigma = S \frac{d\Omega}{\cos^4(\chi/2)}, \quad (9)$$

where

$$S = \left[\frac{Z_c e^2 (m_D + m_C)}{4m_D m_C V^2} \right]^2, \quad (10)$$

and $d\Omega = 2\pi \sin \chi d\chi$ is an element of the solid angle in the velocity space in the COM frame. Note that we consider collisions of the particles with initially the same velocity, so that the COM frame is the same for all colliding pairs of C and D.

From this point on, we will consider a simplified initial value problem, where the streams are uniform in space and are overimposed on each other at $t=0$. Then, the number of scattered deuterons per the solid angle, $F(\chi)$, will grow linearly with time:

$$F(\chi) = \frac{2V n_D n_C S}{\cos^4(\chi/2)} t. \quad (11)$$

The factor of 2 in the numerator appears due to the fact that, before the collision, the carbon and deuterium ions have a relative velocity of $2V$. Here n_D and n_C are the densities of the carbon and deuterium ions per jet. Typically, in the experiments of the type [1] they are equal,

$$n_D = n_C = n. \quad (12)$$

We will assess some of the effects of finite dimensions of the streams in Part 2 of this report.

4. The neutron yield

The number of neutrons produced per unit volume per unit time in this system is

$$\dot{Y} = 2\pi n_D \int_0^\pi \sigma_n(v_{Drel}) v_{Drel} F(\chi) \sin \chi d\chi, \quad (13)$$

where σ_n is a neutron production cross-section [9], v_{Drel} is defined by Eq. (7), and the factor $2\pi \sin \chi d\chi$ comes from the definition of the solid angle.

The fusion reactivity strongly depends on the scattering angle: at small scattering angles, $\pi - \chi \ll 1$, the relative velocity of the scattered deuterons and the main body of un-scattered deuterons is small, and the reactivity drops precipitously (Fig. 2). This allows one to use Eq. (13) for the evaluation of fusion yield related to large-angle scattering events, despite the presence of a formal divergence in F . In reality, these small-angle scattering events with $\chi \rightarrow \pi$ are described by the Landau collision integral and, in the case of rare collisions, cannot cause a strong heating of the interpenetrating streams during a limited time during which they overlap.

An expression for the cross-section for the neutron-generating branch of the DD reaction can be represented as [8]:

$$\sigma_n(\text{barn}) = \frac{19.35}{v_{Drel}^2 (Mm/s) \left[\exp \frac{14.82}{v_{Drel} (Mm/s)} - 1 \right]}. \quad (14)$$

Collecting all the numerical factors in the Eq. (7) for v_{Drel} , we find:

$$v_{Drel} (Mm/s) = 2.42 \sqrt{1 + \cos \chi} V (Mm/s) \quad (15)$$

The reactivity $\sigma_n(v_{Drel}) v_{Drel}$ can then be presented as:

$$\sigma_n(v_{Drel}) v_{Drel} = \frac{79.8 \times 10^{-17} (cm^3/s)}{V (Mm/s) \sqrt{1 + \cos \chi} \left[\exp \left(\frac{6.12}{V (Mm/s) \sqrt{1 + \cos \chi}} \right) - 1 \right]} \quad (16)$$

Equation (16) leads to the plots of Fig. 2.

The factor S (Eq. (10)) of the dimension of cm^2 can be presented numerically as:

$$S(cm^2) = \frac{1.457 \times 10^{-22}}{V(Mm/s)^4}. \quad (17)$$

The distribution function F can be presented numerically as:

$$F(cm^{-3}) = 1.17 \times 10^{-22} \frac{n_D(cm^{-3}) n_C(cm^{-3}) t(ns)}{(1 + \cos \chi)^2 [V(Mm/s)]^3}. \quad (18)$$

Substituting Eqs. (16) and (18) into Eq. (13), one finds the following expression for the yield \dot{Y} :

$$\dot{Y}(cm^{-3}/s) = 10^{-39} [n(cm^{-3})]^3 t(ns) G(V) \quad (19)$$

where we accounted for Eq.(12). The function G has a dimension of cm^6/s^2 and can be evaluated as follows:

$$G(cm^6/s^2) = \frac{584}{[V(Mm/s)]^4} \int_0^\pi \frac{\sin \chi d\chi}{(1 + \cos \chi)^{5/2} \left[\exp \left(\frac{6.12}{V(Mm/s) \sqrt{1 + \cos \chi}} \right) - 1 \right]} \quad (20)$$

Function $G(V)$ is shown in Fig. 3.

5. The neutron yield in the case of two CD streams

For two weakly-to-moderately collisional CD streams the neutrons are generated predominantly in the “beam-beam” collisions between the deuterons of the two streams. Estimates of the neutron yield based on this model provide a reasonable agreement with the experimental data (see Fig. 4). Of course, detailed quantitative comparisons have to use numerical simulations, the would account for the spatio-temporal evolution of the flow.

Our approach, however, is to evaluate the neutron yield in the initial-value problem for two uniform streams superimposed on each other at $t=0$, in other words, in the exactly the same setting as that used in sections 3 and 4. Then, finding the ratio of the two yields, we will eliminate a lot of uncertainties caused by the spatial scales of the interacting streams.

For two identical streams, each having velocity V , we have, instead of Eq. (15),

$$\sigma_n(v_{Drel})v_{Drel} = \frac{0.97 \times 10^{-15}(cm^3/s)}{V(Mm/s) \left[\exp \frac{7.4}{V(Mm/s)} - 1 \right]} \quad (21)$$

The neutron yield per unit volume and unit time will then be

$$\dot{Y}^*(cm^{-3}/s) = 10^{-18} [n(cm^{-3})]^2 H(V), \quad (22)$$

where the asterisk indicates a yield from the beam-beam collisions and $H(V)$ is defined as:

$$H(cm^3/s) = \frac{970}{V(Mm/s) \left[\exp \frac{7.4}{V(Mm/s)} - 1 \right]} \quad (23)$$

6. Comparing the neutron yields

We can now get an idea of the relative role of the knock-on deuterons in the generation of the neutrons. Note that an accurate assessment of the problem would require accounting for the spatio-temporal characteristics of the colliding streams and the related spatio-temporal evolution of the distribution function of the knock-on deuterons.

We will discuss several aspects of this problem in the Part 2 of this report, but

here we will focus on the *ratios* of the two sources of the neutrons. This would make the comparison of the two sources much less sensitive to the aforementioned “form-factors”. So, based on Eqs. (19) and (22) we will find the ratio of Y to Y^* . When making this comparison, one has to remember that the instantaneous yield \dot{Y} grows linearly with time since the moment when the streams have been superimposed. So, the instantaneous yield Y grows as $Y = \dot{Y}t / 2$; the instantaneous yield \dot{Y}^* is constant, and $Y^* = \dot{Y}^* t$. This leads to the following result:

$$\frac{Y}{Y^*} = 5 \times 10^{-22} t(ns) n(cm^{-3}) Q[V(Mm/s)], \quad (24)$$

where the function Q of the dimension cm^3/s is

$$Q = \frac{G}{H}. \quad (25)$$

The plot of the function Q is shown in Fig. 5.

Consider as a reference the case where the characteristic flow velocity is $V=1Mm/s$ – a typical value for the experiments of the type [1]. For this V , the Q is 3.29, so that

$$\frac{Y}{Y^*} = 1.64 \times 10^{-21} t(ns) n(cm^{-3}). \quad (26)$$

One sees that for the typical ion densities ($2 \times 10^{19} cm^{-3}$) and overlap durations (3 ns) the contribution to the yield from the large-angle scattering can be non-negligible and deserves a more careful analysis.

In Part 2 of this report possible experimental signatures of this process will be discussed.

References

1. Hye-Sook Park, D.D. Ryutov, J.S. Ross, N.L. Kugland, S.H. Glenzer, C. Plechaty, S.M. Pollaine, B.A. Remington, A. Spitkovsky, L. Gargate, G. Gregori, A. Bell, C. Murphy, Y. Sakawa, Y. Kuramitsu, T. Morita, H. Takabe, D.H. Froula, G. Fiksel, F. Miniati, M. Koenig, A. Ravasio, A. Pelka, E. Liang, N. Woolsey, C.C. Kuranz, R.P. Drake, M.J. Grosskopf “Studying astrophysical collisionless shocks with counterstreaming plasmas from high power lasers,” *High Energy Density Physics*, **8**, 38, January 2012.
2. D.D. Ryutov. "Self-purification of a fusion plasma in a tandem mirror". *Sov.J. Plasma Phys.*, **13**, 741 (1987).
3. D.D. Ryutov. "Energetic ion population formed in close collisions with fusion alpha-particles". *Physica Scripta*, **45**, 153-158 (1992).
4. R.K. Fisher, P.B. Parks, J.M. McChesney, M.N. Rosenbluth. “Fast alpha-particle diagnostics using knock-on ion tails.” *Nucl. Fusion*, **34**, 1291 (1994).
5. V.G. Nesenevich, V.I. Afanasyev, P.R. Goncharov et al. “Use of neutralized knock-on ion fluxes for alpha-particle confinement studies.” *Plasma Phys. Controlled Fusion*, **56**, 125002 (2014).

6. A. E. Turrell, M. Sherlock, S.J. Rose. “Effects of Large-Angle Coulomb Collisions on Inertial Confinement Fusion Plasmas.” Phys. Rev. Lett., **112**, 245002 (2014).
7. A. E. Turrell, M. Sherlock, S.J. Rose. “Self-consistent inclusion of classical large-angle Coulomb collisions in plasma Monte Carlo simulations.” J. Comp. Phys., JOURNAL OF COMPUTATIONAL PHYSICS Volume: **299**, 144 (2015).
8. L. D. Landau and E.M. Lifshitz. “Mechanics,” Pergamon Press, 1976.
9. D.L. Book. NRL Plasma Physics Formulary. NRL, 1987

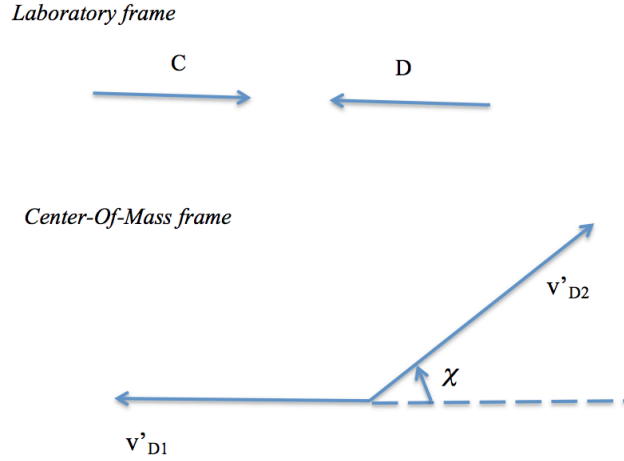


Fig.1 Collision kinematics in the Center-Of-Mass frame. At the top the Lab frame is used; the carbon and deuterium ions are approaching each other with the same velocity V . At the bottom, the scattering of the deuterium ion in the Center-Of-Mass frame is shown; the scattering center in this frame is at rest; the deuterium ion velocity does not change, just turns by some angle χ . Note the definition of χ : it is zero when the scattered ion is moving oppositely to the incoming one; for small angle scattering χ is close to π .

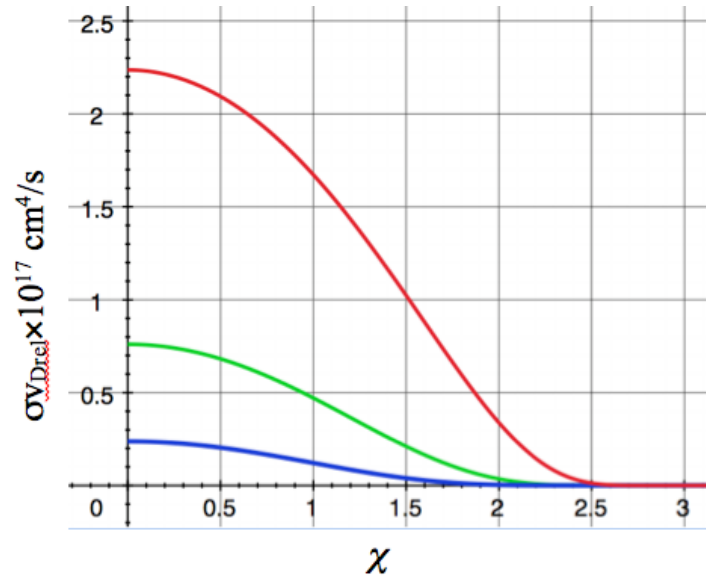


Fig. 2 Reactivity for the knock-on deuterons. Red curve: $V=1.5 \text{ Mm/s}$; green curve: $V=1 \text{ Mm/s}$; blue curve: $V=0.75 \text{ Mm/s}$.

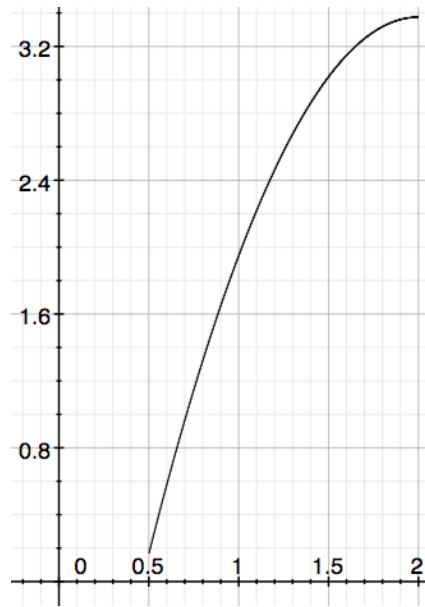


Fig. 3 Function $G(V)$

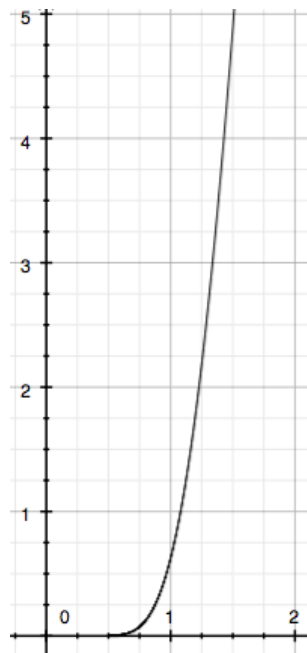


Fig.4 Function $H(V)$

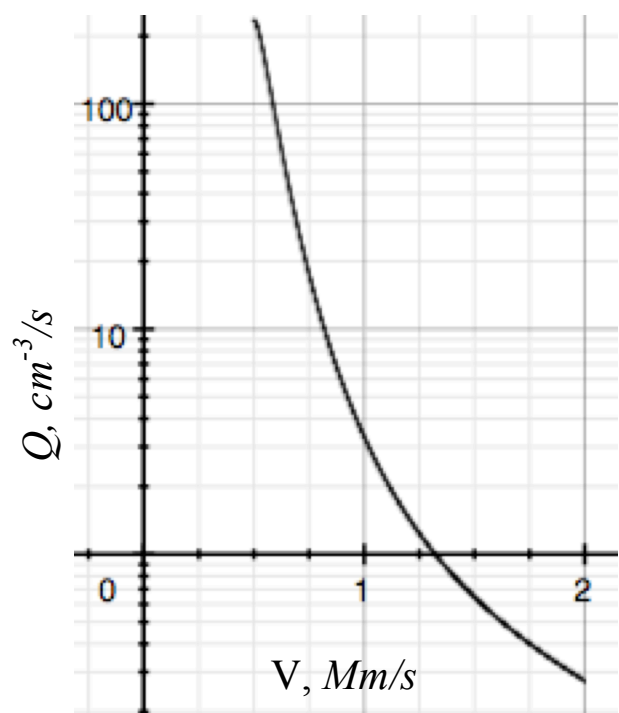


Fig. 5 Function $Q(V)$